SI - On-off mobilization of contaminants in soils during redox oscillations

Supporting Information to "On-off mobilization of contaminants in soils during redox oscillations"

Raoul-Marie Couture†‡*#, Laurent Charlet♮#, Ekaterina Markelova‡♮, Benoît Madé†, Christopher T. Parsons♮‡*#

†Norwegian Institute for Water Research, Gaustadalléen 21, 0349 Oslo, Norway

‡Ecohydrology Group, Department of Earth and Environmental Sciences, University of Waterloo, 200 University Ave. W, Waterloo, ON N2L 3G1, Canada

♮ISTerre, Université of Grenoble 1 and CNRS, P.O. Box 53, F 38041 Grenoble, France

†Andra, National Radioactive Waste Management Agency, R&D Division, Transfer Migration Group, 1/7 rue Jean Monnet, 92298 Chatenay Malabry Cedex, France

*Corresponding authors: Chris Parsons (chris.parsons@uwaterloo.ca), phone: +1 519 888-4567 ext. 32820, and Raoul-Marie Couture (rmc@niva.no), phone: +47 98286478

# Couture, Charlet and Parsons contributed equally to the work.

16 pages, 7 Tables, and 6 Figures

Table of content:

SI - On-off mobilization of contaminants in soils during redox oscillations

1. **Details on the redox-oscillating reactor (ROR) setup**

A custom two part Pyrex® glass redox stat reactor system was used, previously described in Parsons, et al. (2013)[1]. The E_H and pH electrode signals were connected to FET instrumentation amplifiers with high input impedance. The signal was then passed to an Agilent acquisition/switching unit (34970a) connected to a PC running Agilent BenchLink Data Logger 3 software. E_H and pH data were recorded every 5 minutes and the sparging gas was modulated between N_2:CO_2 (392 ppmv) and compressed air via the Agilent switching unit, a relay board and a system of solenoid valves.

The lower part of the reactor (Ace-Glass Inc, NJ, USA) contained a working volume of 1 L and used a water jacket to allow for precise temperature control. Ethylene glycol was added to the temperature regulating circuit to avoid fungal and bacterial growth. The upper part of the reactor contained a headspace volume of approximately 300 mL and used ace-glass threaded connections for sampling, electrodes and mechanical agitation (seals secure up to 2.4 bar of internal/external pressure difference). The agitation shaft and blades were Teflon coated and prior to the introduction of soil suspensions the reactor and all glass and plastic parts were washed with 5% HNO3 then rinsed thoroughly in 18.2 MΩ cm^{-1} water.

Solid polymer open junction Xerolyt electrodes (Mettler-Toledo, France) were selected for their long-term stability and low electrolyte leak rates. A five point calibration was performed for the pH electrodes at the start and end of the experiment showing that electrode response had not shifted more than 0.02 pH units during the experiments. Measured E_H readings were converted to a redox potential with respect to the Standard Hydrogen Electrode (SHE) by normalization using ZoBell's solution. The calculated difference at the start of experiments was equal to the electrode manufacturer specification of 207 mV. The E_H electrode was found to drift by 4 mV during the experiments.

SI - On-off mobilization of contaminants in soils during redox oscillations

2. Soil characterization and preparation

Table SI-1. ICP-MS elemental analysis on initial soil after acid-digestion

Element	Total concentration (mg kg^{-1})
Cr	65.8
Mn	2900
Fe	92400
As	29
Se	$0.1 < x < 1$
Cd	0.415
U	3.12
Sb	ND

Table SI-2. Water content, pH, carbon and particle size analysis*

Measurement	Value	Units
Water Content	19.22	%
pH	8.3	
Organic Carbon	12.1	g kg^{-1}
CaCO$_3$ total	100	g kg^{-1}
Clay (<2 µm)	94	g kg^{-1}
Fine Silt (2−32 µm)	120	g kg^{-1}
Coarse Silt (32−63 µm)	136	g kg^{-1}
Fine Sand (63−500 µm)	400	g kg^{-1}
Coarse Sand (500−2000 µm)	150	g kg^{-1}

*By sieving and sedimentation and after decarbonisation

Soil preparation: The field moist soil was removed from polyethylene sampling bags and suspended in river water to provide a background electrolyte mix and avoid osmotic shock to the microbial community. The concentration of the suspension was approximately 150 g/L (dry-weight equivalent). The suspension was shaken for 5 minutes in a polyethylene bottle and then passed through a <600 m sieve to remove larger rock fragments and large solid organic material. This procedure was repeated until a homogeneous suspension was achieved. The dry weight was then re-determined, and the 150 g/L solution was diluted with MQ water to a precise final concentration of 100 g/L. The resulting suspension was agitated on a shaker and left to equilibrate for 5 days prior to reactor experiments.
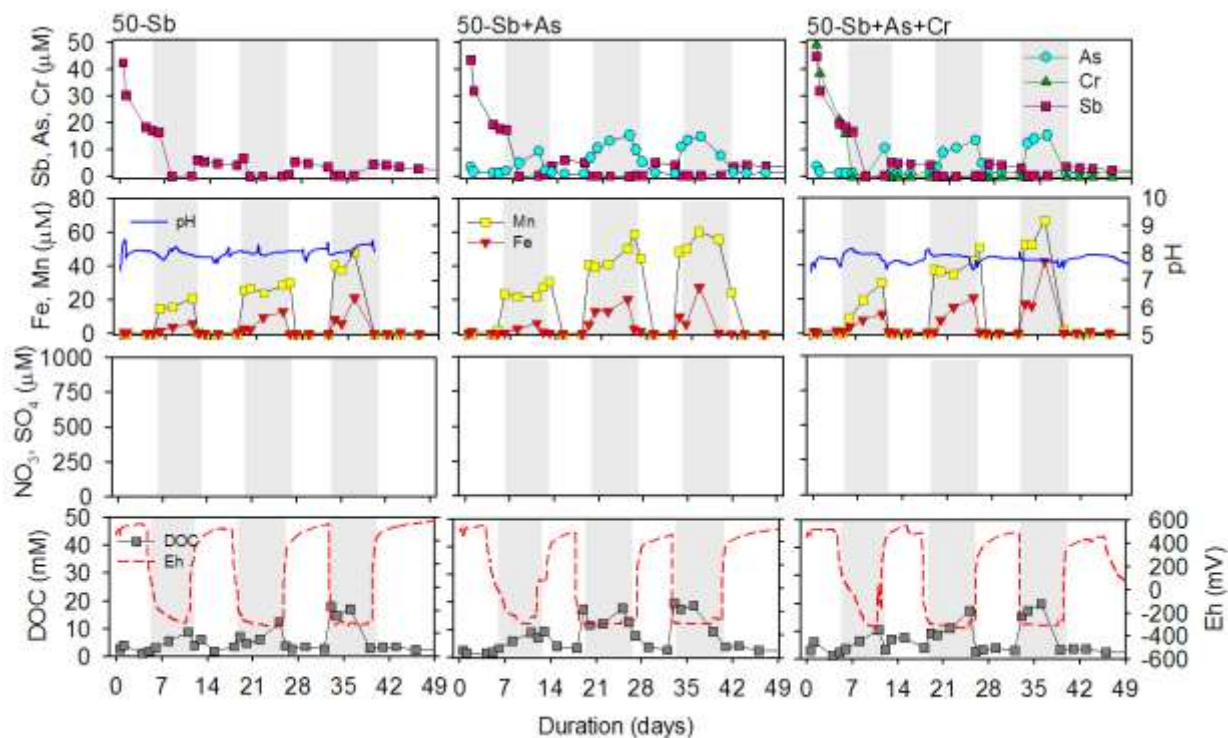
3. Complete dataset for all experiments.
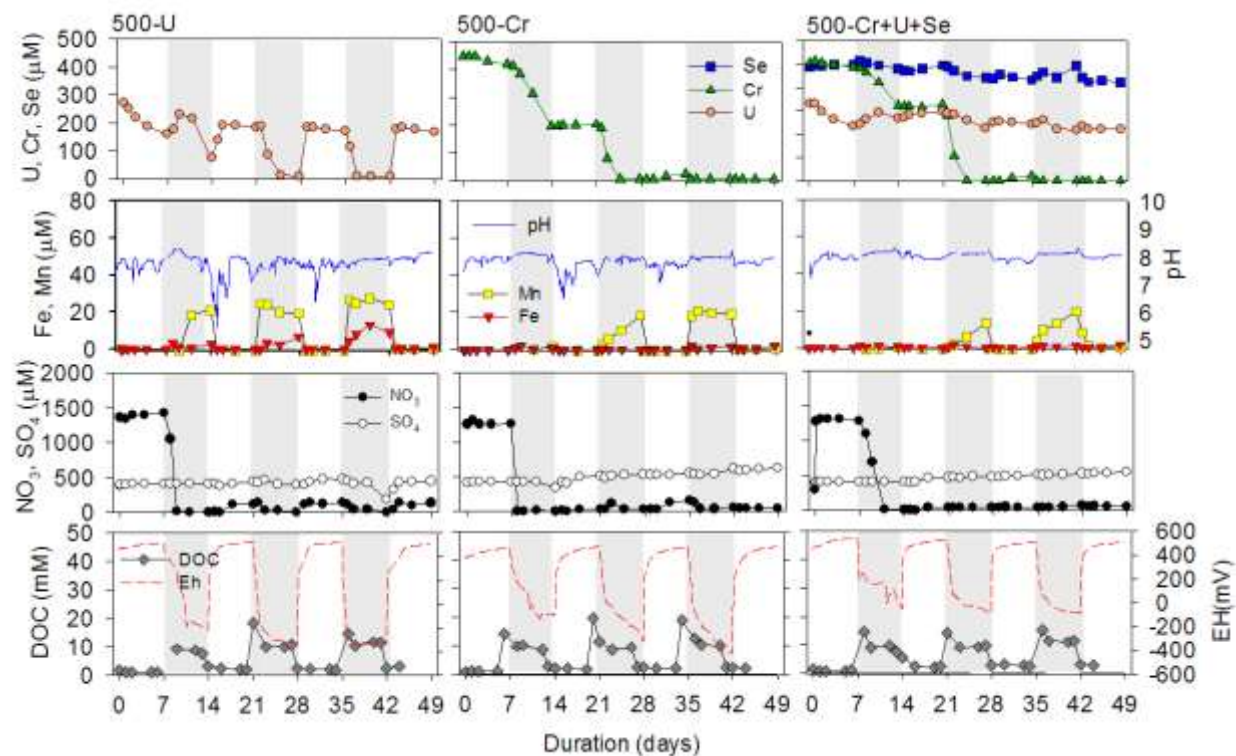

Figure SI-1. Measured time-series of As^V (open squares), As^{III} (open diamonds), Se (dark squares), Mn (light squares), Fe (downward triangles), NO_3^- (solid circles), SO_4^{2-} (open circles), DOC (dark squares), and E_H (line) during 7 consecutive experimental half-cycles for experiments 0-Soil, 500-As and 500-Se. Shaded areas indicate half-cycles during which an anoxic headspace was imposed. Only As was measured during the "Soil only" experiment, with concentrations consistently < 1 μM.

Figure SI-2. Measured time-series of Sb (solid diamonds), As (light circles), Cr (upward triangles), Mn (light squares), Fe (downward triangles), DOC (dark squares), and E_H (line) during 7 consecutive experimental half-cycles for experiments 50-Sb, 50-Sb+As and 50-Sb+As+Cr. Shaded areas indicate half-cycles during which an anoxic headspace was imposed. Samples for NO_3^- and SO_4^{2-} could not analyze for these experiments due to instrument downtime.

Figure SI-3. Measured time-series of U (circles), Cr (upward triangles), Se (blue squares), Mn (light squares), Fe (downward triangles), NO_3^- (solid circles), SO_4^{2-} (open circles), DOC (dark squares), and E_H (line) during 7 consecutive experimental half-cycles for experiments 500-U, 500-Cr and 500-Cr+Se+U. Shaded areas indicate half-cycles during which an anoxic headspace was imposed.

4. Supporting information on model rates and constants.

Table SI-3. Redox reactions, their theoretical equilibrium redox potentials (E_H^0, in volts relative to the standard hydrogen electrode) and corresponding pe for dominant species at standard state and at pH 7.5. For the calculations at pH 7.5, concentrations of 5×10^{-4} M are set for Cr, Mn, U, Se, Sb, As, Fe and C. Fe and Mn are in equilibrium with ferrihydrite and birnessite, respectively, and the aqueous concentrations for Fe^{II} and Mn^{II} were set to 1×10^{-6} M.

Reaction	E_H^0 pH = 7.5	$pe^{7.5}$	E_H^0 pH = 0	pe^0	Log K	ref.
$O_2 + 4H^+ + 4e^- = 2H_2O$	0.77	13.11	1.22	20.78	83.12	[2]
$MnO_{2(s)} + 4H^+ + 2e^- = Mn^{2+} + 2H_2O$	0.55	9.44	1.22	20.8	41.60	[2]
$CrO_4^{2-} + 8H^+ + 3e^- = Cr^{3+} + 4H_2O$	0.43	7.39	1.51	25.66	77.00	[2]
$SeO_4^{2-} + 2e^- + 3H^+ = HSeO_3^- + H_2O$	0.40	6.85	1.07	18.16	36.32	[2]
$HSeO_3^- + 5H^+ + 4e^- = Se^0_{(s)} + 3H_2O$	0.16	2.74	0.77	14.8	59.2	[2]
$SbO_3^- + 3H^+ + 2e^- = Sb(OH)_3^0$	-0.03	-0.45	0.76	11.3	24.31	[2]
$UO_2^{2+} + 2e^- = UO_{2(s)}$	-0.06	-1.14	0.19	-3.3	16.22	[3]
$AsO_4^{3-} + 2H^+ + 2e^- = AsO_3^{3-} + H_2O$	-0.06	-1.15	0.15	2.64	5.29	[2]
$Fe(OH)_{3(s)} + 3H^+ + e^- = Fe^{2+} + 3H_2O$	-0.17	-2.97	0.67	11.31	17.1	[2]
$2CO_2 + 12H^+ + 12e^- = C_2H_5OH + 3H_2O$	-0.35	-5.99	0.09	1.52	33.93	[5]

Table SI-4. Kinetic Formulations Used in the Model.

Description	Reaction	Kinetic formulation	Rxn ID
Aerobic respiration	$CH_2O + O_2 \rightarrow CO_2 + H_2O$	Roxy = k_om×[CH₂O]×f_o2	1
Cr(VI) bioreduction	$3CH_2O + 4CrO_4^{2-} + 16H+ \rightarrow 4Cr(OH)^{2+} + 3CO_2 + 9H_2O$	Rcr = k_om×[CH₂O]×f_cr	2
Mn(IV) oxide bioreduction	$CH_2O + 4MnO_2 \rightarrow 4Mn^{3+} + CO_2 + H_2O$	Rmnox = k_om×[CH₂O]×f_mnox	3
Fe(III) oxide bioreduction	$CH_2O + 4Fe(OH)_3 + 8H^+ \rightarrow 4Fe^{2+} + CO_2 + 11H_2O$	Rhfo = k_om×[CH₂O]×f_hfo	4
Oxidation of Fe(II)	$Fe^{2+} + 0.25O_2 + H^+ \rightarrow Fe^{3+} + 0.5H_2O$	Rfeox = k_feox×[O₂]×[Fe⁺²]	5
Se(IV) bioreduction	$HSeO_3^- + 5H^+ + 4e^- \rightarrow Se^0_{(s)} + 3H_2O$	Rse = k_se_zero × [HSeO₃-]	6
Se(0) oxidation	$Se^0_{(s)} + 3H_2O \rightarrow HSeO_3^- + 5H+ + 4e^-$	R_se = k_seox × [O₂]	7

Where:

f_o2 = [O2]/[O2]+Km_o2

f_cr = ([CrO4-2]/([CrO4-2]+Km_cr)) + (Kin_o2/(Kin_o2+[O2]))

f_mnox = ([MnO2]/([MnO2]+Km_mn)) + (Kin_o2/(Kin_o2+[O2])) + (Kin_cr/(Kin_cr+[CrO2+2]))

f_hfo = ([CrO4-2]/([CrO4-2]+Km_fe)) + (Kin_o2/(Kin_o2+[O2])) + (Kin_cr/(Kin_cr+[CrO2+2])) + (Kin_mnox/(Kin_mnox+[MnO2]))

SI - On-off mobilization of contaminants in soils during redox oscillations

Table SI-5. Reaction parameters constrained by the model which correspond to reactions #1-7 given in Table SI-4 and to reaction #28 in Table SI-6.

Parameter	Abbrev.	Value	Unit	Source	Range	Ref.
OM oxidation rate constant	k_om	20	yr^{-1}	M	1-400	[6]
Half-saturation value for oxic respiration	Km_o2	5	$\mu mole\ L^{-1}$	L	4–8	[7, 8]
Inhibition of TEAs by O_2	Kin_o2	1	$\mu mole\ L^{-1}$	L	3.2×10^{-3}–1	[7, 8]
Half-saturation for Cr reduction	Km_cr	1	$\mu mole\ L^{-1}$	L	0–1	[9]
Inhibion of TEAs by Cr	Kin_cr	3	$\mu mole\ L^{-1}$	M		
Half-saturation for Mn reduction	Km_mn	15	$\mu mole\ L^{-1}$	L	16	[10]
Inhibition of TEAs by Mn	Kin_mn	500	$\mu mole\ L^{-1}$	M		
Half-saturation for Fe reduction	Km_fe	1	$\mu mole\ L^{-1}$	L	0.2–200	[7, 8]
Rate constant for Fe oxidation by O_2	k_feox	4	$L\ \mu mole^{-1}\ s^{-1}$	L	3.5–40	[7, 8]
Equilibrium constant for Fe	k_fe_exch	-2.5		L	-2–-3	[11]
Rate constant for Se^0 precipitation	k_se_zero	7×10^{-6}	s^{-1}	M		
Rate constant for Se^0 oxidation by O_2	k_seox	1.5	$L\ \mu M^{-1}\ s^{-1}$	L	$1–3000\ s^{-1}$	[12]

M = model fit, L = literature value

Table SI-6. Reactions for the formation of the various oxyanion species and their corresponding equilibrium constants added to the WATEQ4F database in PHREEQC. Solid phases allowed to form in the model are also listed.

Reaction	Log K	Ref.	Rxn ID
Surface complexation reactions			
$Hfo\_wOH + CO_3^{-2} + H^+ = Hfo\_wOCO_2^- + H_2O$	12.78	[13]	8
$Hfo\_wH + CO_3^{-2} + 2H^+ = Hfo\_wOCO_2H + H_2O$	20.37	[13]	9
$Hfo\_sOH + Fe^{+2} = Hfo\_sOFe^+ + H^+$	−0.95	[13]	10
$Hfo\_wOH + Fe^{+2} = Hfo\_wOFe^+ + H^+$	−2.98	[14]	11
$Hfo\_wOH + Fe^{+2} + H_2O = Hfo\_wOFeOH + 2H^+$	−11.55	[14]	12
$Hfo\_OH + AsO_4^{-3} + 2H^+ = Hfo\_HAsO_4^- + H_2O$	24.4	[15]	13
$Hfo\_OH + AsO_4^{-3} + H^+ = Hfo\_AsO_4^{-2} + H_2O$	18.1	[15]	14
$Hfo\_OH + AsO_3^{-3} + 3H^+ = Hfo\_H_2AsO_4^{-2} + H_2O$	38.8	[15]	15
$Hfo\_OH + AsO_3^{-3} + 2H^+ = Hfo\_HAsO_4^{-2} + H_2O$	31.9	[15]	16
$2Hfo\_sOH + Sb(OH)_6^- = (Hfo\_sO)_2Sb(OH)_4^- + 2H_2O$	13	[16]	17
$2Hfo\_sOH + Sb(OH)_3 = (Hfo\_sO)_2Sb(OH) + 2H_2O$	15	[16]	18
$2Hfo\_wOH + Sb(OH)_6^- = (Hfo\_wO)_2Sb(OH)_4^- + 2H_2O$	5	[16]	19
$2Hfo\_wOH + Sb(OH)_3 = (Hfo\_wO)_2Sb(OH) + 2H_2O$	6	[16]	20
$Hfo\_sOH + UO_2^{+2} = Hfo\_sOUO_2^+ + H^+$	1.74	[17]	21
$Hfo\_wOH + UO_2^{+2} = Hfo\_wOUO_2^+ + H^+$	1.54	[17]	22
Solid phases			
$Cr(OH)_3$	1.34	[18]	24
$Sb(OH)_{3(aq)} = Sb(OH)_{3(s)}$	−7.11	[18]	25
$U^{4+} + 2H_2O = UO_{2(s)} + 4H^+$	−4.67	[18]	26
Cation exchange			
$X^- + H^+ = XH$	3	[11]	27
$Fe^{+2} + XH = FeX^+ + H^+$	−2.5	[11]	28

5. Model code

The model code is available online at https://github.com/biogeochemistry/ROR-phreeqc. To gain access to the repository please email your GitHub username to rmc@niva.no.The structure of the code is sumarized on Figure SI-4.

```
4    ### SIMULATION 1 ###
5
6    SOLUTION_MASTER_SPECIES
7    SURFACE_SPECIES
8    SOLUTION_SPECIES
9    PHASES
10   EXCHANGE_MASTER_SPECIES
11   EXCHANGE_SPECIES
12   SOLUTION 0
13   EQUILIBRIUM_PHASES 0
14   EXCHANGE 0
15   SAVE SOLUTION 0;SAVE EXCHANGE 0; SAVE EQUILIBRIUM_PHASES 0;
16   END
17
18   # KINETIC MODEL PARAMETER #
19
20   RATES
21   [...]
22
23   # OUTPUT CONFIGURATION #
24   USER_GRAPH
25   INCREMENTAL_REACTIONS true ;
26
27   # REDOX CYCLING  #
28
29   ### SIMULATION 2 ###
30   TITLE 0.5 CYCLE OXIC
31   USE SOLUTION 0 ; USE EXCHANGE 0; USE EQUILIBRIUM_PHASES 0;
32   GAS_PHASE;
33   KINETICS 0
34   SURFACE 0
35   SAVE SOLUTION 0;SAVE EXCHANGE 0; SAVE EQUILIBRIUM_PHASES 0; SAVE  SURFACE 0
36   END
37
38   ### SIMULATION 3 ###
39   TITLE MIXING A DOC SPIKE WITH THE RESULT OF SIMULATION 0
40   SOLUTION 1
41   MIX 1;
42   SAVE SOLUTION 0
43
44   ### SIMULATION 4 ###
45   TITLE 1.0 CYCLE ANOXIC
46   USE SOLUTION 0 ; USE EXCHANGE 0; USE EQUILIBRIUM_PHASES 0; USE  SURFACE 0;
47   GAS_PHASE;
48   KINETICS 1
49   SAVE SOLUTION 0;SAVE EXCHANGE 0; SAVE EQUILIBRIUM_PHASES 0; SAVE  SURFACE 0
50   END
51
52   [...]
53
54
55
```
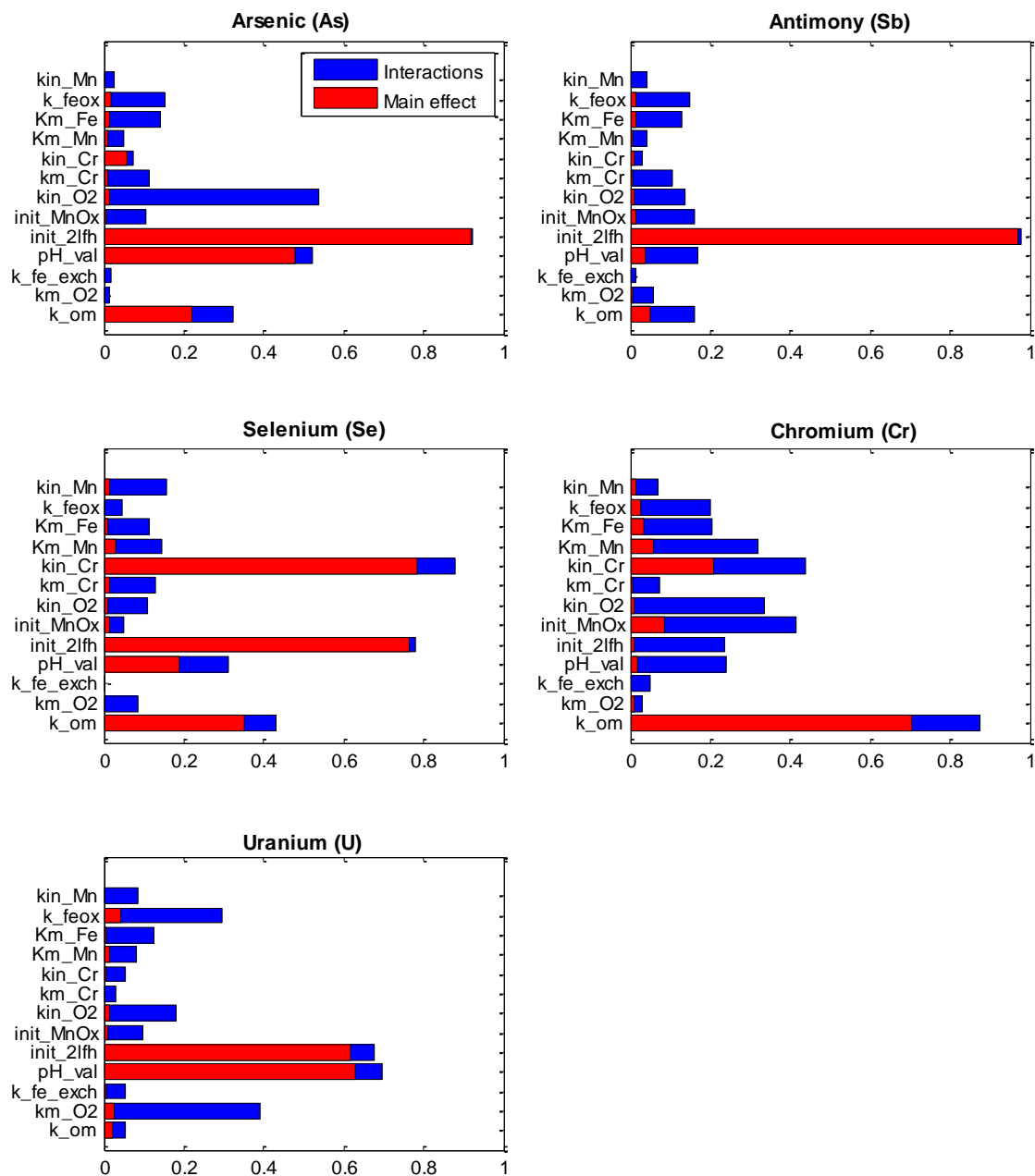
Figure SI-4. Sequence of the PHREEQC v3 section headings and keywords used to simulate element behavior during redox oscillations and produce Figures 2 & 3 of the main text.

6. Model sensitivity analysis and performance metrics

Figure SI-5. Proportion of total variance in modeled aqueous concentrations of As, Sb, Se, Cr and U explained by 10 parameters analyzed by the Extended Fourier amplitude sensitivity test (Extended FAST) sensitivity analysis method. "Main effect" denotes the part of total variance explained by a single parameter and "Interactions" the part explained by interactions with all other parameters. Parameter abbreviations are explained in Table SI-2.

Figure SI-6. Proportion of total variance in modeled aqueous concentrations of As, Sb, Se, Cr and U explained by 13 parameters analyzed by the Extended Fourier amplitude sensitivity test (Extended FAST) sensitivity analysis method. "Main effect" denotes the part of total variance explained by a single parameter and "Interactions" the part explained by interactions with all other parameters. Parameter abbreviations are explained in Table SI-2.

Table SI-7. Pearson's correlation coefficient (r), root-mean-square error (RMSE), observation standard deviation (σ_{obs}) and RMSE:σ_{obs} ratio (RSR) calculated using modeled and measured contaminant concentrations time-series.

Element (50 µM)	Sb	As	Cr	Mn	Fe	C
r	0.61	0.89	0.91	0.92	0.65	0.89
RMSE	6.9**	2.9	8.5*	11.1	7.5	3.3
σ	7.7	5.2	12.6	28.1	8.5	5.3
RSR	0.89	0.56	0.67	0.40	0.88	0.61

Element (500- µM)	Cr	Se	U	Mn	Fe	C
r	0.99	0.99	0.75	0.81	0.81	0.90
RMSE	0.02	0.03	0.06	13.1	5.2	3.5
σ	0.18	0.23	0.07	9.4	2.5	6.8
RSR	0.11	0.14	0.94	1.40	2.07	0.52

* RMSE = 0.07 if the 1st oxic half-cycle is excluded
**RMSE = 2 if the 1st oxic half-cycle is excluded

SI - On-off mobilization of contaminants in soils during redox oscillations

Litterature Cited

1.   Parsons, C. T.; Couture, R.-M.; Omoregie, E. O.; Bardelli, F.; Greneche, J.-M.; Roman-Ross, G.; Charlet, L., The impact of oscillating redox conditions: Arsenic immobilisation in contaminated calcareous floodplain soils. *Environ. Pollut.* **2013,** *178* (0), 254-263.

2.   Brezonik, P. L.; Arnold, W. A., *Water Chemistry: An Introduction to the Chemistry of Natural and Engineered Aquatic Systems*. Oxford University Press: New York, 2011.

3.   Chappaz, A.; Gobeil, C.; Tessier, A., Controls on uranium distribution in lake sediments. *Geochim. Cosmochim. Acta* **2010,** *74* (1), 203-214.

4.   Kirk, G., Reduction and Oxidation. In *The Biogeochemistry of Submerged Soils*, John Wiley & Sons, Ltd: 2004; pp 93-134.

5.   Canfield, D.; Kristensen, E.; Thamdrup, B., *Aquatic Geomicrobiology*. Elsevier Academic Press: San Diego, USA, 2005; Vol. 48, p 656.

6.   Paraska, D. W.; Hipsey, M. R.; Salmon, S. U., Sediment diagenesis models: Review of approaches, challenges and opportunities. *Environ. Model. Soft.* **2014,** *61*, 297-325.

7.   Canavan, R. W.; Slomp, C. P.; Jourabchi, P.; Van Cappellen, P.; Laverman, A. M.; Van Den Berg, G. A., Organic matter mineralization in sediment of a coastal freshwater lake and response to salinization. *Geochim. Cosmochim. Acta* **2006,** *70* (11), 2836-2855.

8.   Couture, R. M.; Shafei, B.; Van Cappellen, P.; Tessier, A.; Gobeil, C., Non-Steady State Modeling of Arsenic Diagenesis in Lake Sediments. *Environ. Sci. Technol.* **2010,** *44* (1), 197–203.

9.   Jamieson-Hanes, J. H.; Amos, R. T.; Blowes, D. W., Reactive Transport Modeling of Chromium Isotope Fractionation during Cr(VI) Reduction. *Environ. Sci. Technol.* **2012**.

10.   Van Cappellen, P.; Wang, Y., Cycling of iron and manganese in surface sediments: a general theory for the coupled transport and reaction of carbon, oxygen, nitrogen, sulfur, iron, and manganese. *Am. J. Sci.* **1996,** *296* (3), 197-243.

11.   Appelo, C. A. J.; Postma, D., Ion Exchange. In *Geochemistry, Groundwater and Pollution, Second Edition*, Taylor & Francis: 2005; pp 241-309.

12.   Dowdle, P. R.; Oremland, R. S., Microbial Oxidation of Elemental Selenium in Soil Slurries and Bacterial Cultures. *Environ. Sci. Technol.* **1998,** *32* (23), 3749-3755.

13.   Appelo, C. A. J.; Van der Weiden, M. J. J.; Tournassat, C.; Charlet, L., Surface Complexation of Ferrous Iron and Carbonate on Ferrihydrite and the Mobilisation of Arsenic. *Environ. Sci. Technol.* **2002,** *36* (14), 3096-3103.

14.   Liger, E.; Charlet, L.; Van Cappellen, P., Surface catalysis of uranium(VI) reduction by iron(II). *Geochim. Cosmochim. Acta.* **1999,** *63* (19–20), 2939-2955.

15.   Dixit, S.; Hering, J. G., Comparison of arsenic(V) and arsenic(III) sorption onto iron oxide minerals: Implications for arsenic mobility. *Environ. Sci. Technol..* **2003,** *37* (18), 4182-4189.

16.   Vithanage, M.; Rajapaksha, A. U.; Dou, X. M.; Bolan, N. S.; Yang, J. E.; Ok, Y. S., Surface complexation modeling and spectroscopic evidence of antimony adsorption on iron-oxide-rich red earth soils. *J. Colloid Interf. Sci.* **2013,** *406*, 217-224.

17.   Mahoney, J. J.; Cadle, S. A.; Jakubowski, R. T., Uranyl Adsorption onto Hydrous Ferric Oxide—A Re-Evaluation for the Diffuse Layer Model Database. *Environ. Sci. Technol.* **2009,** *43* (24), 9260-9266.

18.   Parkhurst, D. L.; Appelo, C. A. J., Description of input and examples for PHREEQC version 3—A computer program for speciation, batch-reaction, one-dimensional transport, and

inverse geochemical calculations. In *U.S. Geological Survey Techniques and Methods*, available only at http://pubs.usgs.gov/tm/06/a43/. 2013; pp 1-497.